

Using the Factor Separation Method for land-use land-cover change impacts on weather and climate process with the Regional Atmospheric Modeling System

Beltrán-Przekurat¹, A., R.A. Pielke Sr.¹, J.L. Eastman², G.T. Narisma³, A.J. Pitman⁴, M. Lei⁵ and D. Niyogi⁵

¹ Department of Atmospheric and Oceanic Sciences and Cooperative Institute for Research in Environmental Sciences, 216 UCB, University of Colorado, Boulder, CO 80309

² WindLogics Inc., 201 4th St NW, Grand Rapids, MN 55744

³ Physics Department. Ateneo de Manila University, Loyola Heights, Quezon City, 1108, Philippines

⁴ Climate Change Research Centre, University of New South Wales, Sydney, NSW, 2052, Australia.

⁵ Purdue University, Department of Agronomy, and Department of Earth and Atmospheric Sciences, Lilly Hall of Life Sciences, 915 W. State Street, Purdue University. West Lafayette, IN 47907-2054

Abstract

The use of the Factor Separation Method (FacSep) has been applied effectively in the Regional Atmospheric Modeling System (RAMS) to assess the relative contribution of different factors on weather and climate processes. In this chapter we will discuss model sensitivities to historical and future changes in land use - land cover, biophysical and radiative effects of increased CO₂ concentration and land cover representation assessed using the FacSep in weather and regional climate simulations for various regions around the world. This method emphasizes the importance of land cover changes and CO₂ biological effects when addressing regional-scale future climate change impacts.

Key words: Land-atmosphere interactions; land-use/land-cover change; regional climate; numerical modeling

1. Introduction

Observations and modeling studies show that land-surface properties can influence the near surface-atmosphere through exchanges of heat, moisture, momentum, gases, and aerosols on timescales ranging from seconds to years, and on local to regional and possibly global spatial scales (Pielke, 2001; Arora, 2002; Pielke et al., 2002; Pitman, 2003; Niyogi et al. 2004; Foley et al., 2005). Urbanization, deforestation-reforestation, conversion of natural areas to agriculture, and increases in irrigation areas are some land-cover land-use modifications that often affect albedo, leaf area, roughness length, and root biomass. These landscape modifications can lead to changes in near-surface fluxes that affect temperature (e.g., Baidya Roy et al., 2003; Strack et al., 2008), humidity (e.g., Douglas et al., 2006, 2009; Roy et al., 2007), boundary layer process, and precipitation (Pielke et al., 2007). These changes can potentially feed back to the biophysical variables through a two-way interaction, enhancing or decreasing the initial perturbation (Pitman, 2003; Pielke and Niyogi, 2008).

Increase in atmospheric carbon dioxide (CO_2) concentrations is another process that alters near-surface temperatures (Solomon et al., 2007). The biological response to increases in CO_2 includes a decrease in stomatal conductance (g_s), an increase in carbon assimilation, biomass and leaf area index (LAI) (Cao et al., 2009). Changes in g_s and LAI affect the energy partition between sensible and latent heat, through the transpiration process, which in turn affects soil thermodynamics and eventually near-surface temperature and humidity (Niyogi et al., 2009).

Complex nonlinear interactions between atmosphere and biosphere under land-cover changes (LCC) and increasing CO_2 levels occur at a wide range of spatial scales,

global (e.g. Chase et al., 2001) to regional (e.g. Eastman et al., 2001), and temporal scales, decadal to monthly (e.g. Narisma and Pitman, 2004; Alpert et al. 2007). A key aspect in the understanding of how those processes may affect the climate system is to be able to recognize the underlying mechanisms of the effects induced by each of the factors separately or by their interactions on near-surface atmospheric circulation. The Factor Separation (FacSep) methodology (Stein and Alpert, 1993) can be used to assess the contributions of each of the factors separately and also their synergistic interactions.

In this chapter we review modeling studies that applied the FacSep methodology to assess the relative contribution and the interactions of:

- historical and future changes in land-cover with biophysical and radiative effects of increased CO₂ concentrations (Eastman et al., 2001; Beltrán, 2005; Narisma and Pitman, 2006; Pitman and Narisma, 2005);
- land-cover change patterns (Gero and Pitman, 2006); and
- improved boundary conditions dataset and urban representation (Lei et al., 2008).

The modeling experiments in those studies employed the Regional Atmospheric and Modeling System (RAMS; Pielke et al., 1992; Cotton et al., 2003), coupled with a plant-model (GEMRAMS) and with an urban model (RAMS-TEB) in some of the experiments. These experiments use a wide range of modeling domains, atmospheric boundary conditions and land-cover datasets.

This chapter is organized as follows. A brief description of RAMS, GEMRAMS and RAMS-TEB is provided in Section 2. Applications of the FacSep methodology with RAMS and GEMRAMS for LCC and CO₂ concentration levels are presented in Section

3. Section 4 describes the application of the methodology to evaluate the effects of the spatial pattern of land-cover changes. Section 5 describes how the the FacSep methodology can help to evaluate the relative contributions of model and data improvements. Final comments are presented in Section 6.

2. RAMS, GEMRAMS and RAMS-TEB description

RAMS is a general-purpose, atmospheric-simulation model that includes the equations of motion, heat, moisture, and continuity in a terrain-following coordinate system. It is a fully three-dimensional and non-hydrostatic model. RAMS has been applied to a diverse range of spatial and temporal scales, to study an wide range of processes over domains located all over the world (e.g. Lawton et al., 2001; Cotton et al., 2003 and references therein; De Wekker et al., 2004; Narisma and Pitman, 2004; Beltrán, 2005 and references therein; Douglas et al., 2006, 2009; Roy et al., 2007). RAMS contains several options for the typical physical parameterizations of atmospheric modeling systems. Table 1 shows the options available in the version of the RAMS used in the examples presented in this Chapter.

To analyze the effects of CO₂ on near-surface atmosphere most of the studies discussed in this chapter used the fully coupled atmospheric-plant model version of RAMS that is called GEMRAMS, comprised of the RAMS and the General Energy and Mass Transport Model (GEMTM; Chen and Coughenour, 1994, 2004), an ecophysiological process-based model. One of the main features of GEMRAMS is that the atmosphere and biosphere are allowed to dynamically interact through the surface and

canopy energy balance. Vegetation grows as a function of temperature, radiation, and the water status of the soil and atmosphere. Leaf area index (LAI), computed from leaf biomass, and canopy conductance, estimated from interactions between transpiration, photosynthesis and root-water uptake, are the variables connecting the carbon and energy fluxes components.

GEMTM and the soil-vegetation-atmosphere transfer scheme in RAMS, the Land Ecosystem-Atmosphere Feedback model version 2, LEAF-2, (Walko et al., 2000), connected through LAI and canopy conductance, represent the storage and exchange of heat, moisture, and carbon associated with the near-surface atmosphere and biosphere. At each time step, photosynthesis at the leaf level is calculated for sunlit and shaded leaves and also separately for C₃ and C₄ species (Farquhar et al., 1980; Chen et al., 1994, 1996) as a function of photosynthetic active radiation, temperature and CO₂ concentration. Stomatal conductance for sunlit and shaded leaves is computed using the semi-empirical linear Ball-Berry relationship based on net photosynthesis, relative humidity, and leaf surface CO₂ (Ball et al., 1987). Leaf photosynthesis and conductance are scaled up to the canopy level using sunlit and shaded LAI (Chen and Coughenour, 1994; de Pury and Farquhar, 1997), calculated using light extinction coefficients from a multi-level canopy radiation model (Goudriaan, 1977). The available photosynthate is allocated to leaves, stems, roots, and reproductive organs with variable partition coefficients, which are functions of soil water and temperature conditions. Daily, a new total LAI value is estimated from the daily leaf biomass growth using the vegetation-prescribed specific leaf area.

To study the effects of urbanization on heavy rainfall and surface temperature, Lei et al. (2008) used a version of RAMS coupled to an explicit urban model, the Town Energy Budget TEB (Masson, 2000; Rozoff et al., 2003). TEB follows a generalized urban canyon approach, considering energy budgets separately for roofs, walls, and roads, and also the radiation interactions between those surfaces (Rozoff et al., 2003). Anthropogenic heat release is also incorporated into the TEB.

3. LULC and CO₂ changes

Applications of the FacSep methodology with RAMS and GEMRAMS to study the contributions of LULC and CO₂ changes are given in Eastman et al. (2001), Beltrán (2005), Narisma and Pitman (2006), and Pitman and Narisma (2005).

3.1 Sensitivity to past LULC and CO₂ concentration using current atmospheric conditions

Eastman et al. (2001) considered the effects of three factors, LCC, and radiative and biophysical CO₂ levels, on near-surface atmospheric variables during the 1989 growing season, April to October. The sensitivity experiments were performed over a simulation domain centered on the central Great Plains of the United States. Table 2 summarizes the modeling experiments. The land-cover experiment $\hat{f}1$ corresponds mainly to a conversion from tall and short grasslands to croplands, representing the changes in land-use since pre-settlement to the present. In the CO₂ biology experiment only the CO₂ levels that affect physiological processes, like photosynthesis and

respiration parameterized within GEMTM, were allowed to change. The CO₂ effect on the radiative fluxes corresponded to the CO₂ radiation experiment (Table 2). To isolate the effects of LCC and CO₂ levels, all the simulations used the National Centers for Environmental Prediction-National Center for Atmospheric Research (NCEP-NCAR) reanalysis (Kalnay et al., 1996) as atmospheric boundary conditions.

The results showed that the land-cover and biological CO₂ changes were the dominant factors in the sensitivity experiments (Table 3) over the 7 months simulated. For all the variables analyzed the contribution of the radiative CO₂ changes was minimal. Table 3 shows the seasonal domain-averaged contribution of each of the factors and their interaction to daily maximum (Tmax) and minimum (Tmin) temperature and precipitation (Precip). In the case of Tmax, the contributions of the natural vegetation (\hat{f}_1) and 2xCO₂ biology (\hat{f}_3) by themselves indicate a large cooling effect, of 1.19°C and 0.75°C, representing a 5 and 3% change with respect to the Control experiment (i.e. current land-cover and CO₂ levels). The 2xCO₂ biology (\hat{f}_3) had the largest effect on Tmin, with an average positive change of 4% with respect to the Control experiment.

The interactions among the factors were relatively small in most of the variables, but in the case of Tmin, one of them, the contribution from natural vegetation and 2xCO₂ biology (\hat{f}_{13}) was of the same magnitude than the pure 2xCO₂ radiation effect. Although the \hat{f}_{13} value was small (1% of positive change) this is an indication that the biological effects of increasing CO₂ levels synergistically interact with land-cover changes to affect Tmin: the warming due to the reduction of the long-wave loss, caused by an elevated

near-surface atmospheric water vapor, is compensated by the slight cooling associated with the natural vegetation.

Beltrán (2005) addressed the total LULC and CO₂ changes for a simulation domain covering southern South America (only experiments f0 and f23 were carried out). Here, we present results of additional simulations that complete the set of experiments required by the FacSep methodology, similarly to the modeling approach of Eastman et al. (2001) (Table 2). The simulation experiments were performed for the 1996-1997 austral spring season, September to November.

The lower atmospheric boundary conditions were provided by the European Centre for Medium-Range Weather Forecasts Reanalysis ERA-40 (Uppala et al, 2005). Sensitivity experiments were performed using the current vegetation cover (Figure 1a) and a “historical” one that represents the conditions before European settlement. Croplands were replaced by tall grass, wooded grasslands, or evergreen broadleaf forest, depending on their geographical location based on the vegetation maps of Matthews (1983), Kùchler (2000), and Cabrera and Willink (1980) (Figure 1b). As in Eastman et al. (2001) two CO₂ concentration values, 360 ppm and 720 ppm, were used to address the biological and radiation effects and interactions of increasing CO₂ (Table 2) on near-surface weather variables.

In a domain-averaged basis, the pure and interaction effects in these sensitivity simulations were almost negligible. Nevertheless, spatial differences were noticeable. The contributions of LULC (\hat{f}_1) and increased CO₂ values in the biophysical processes (\hat{f}_3) showed the largest effect on the analyzed variables, mostly associated with changes near-surface latent and sensible heat flux. For example, for the October-November

period, T_{max} was up to 1.2°C higher with a natural vegetation landscape than with the current vegetation in areas where vegetation changed from C_3 grasslands to wheat and soybean (i.e. in central and southern Pampas), and was up to 0.3°C lower when crops replaced evergreen trees (e.g., in southern Brazil) (Figure 2). The contribution from the CO_2 biophysical changes (\hat{f}_3) showed T_{max} increases of up to 0.4°C in areas associated with an increase in LAI values (Figure 2). Interestingly the interaction term \hat{f}_{13} that represents the contributions from natural vegetation and $2\times\text{CO}_2$ biology has a negative effect on T_{max} in the southern Pampas. T_{max} is still higher in the f_{13} experiment (i.e. natural vegetation and $2\times\text{CO}_2$ biology) than in the control run with current vegetation, f_0 , but the its combined effect on T_{max} is lower than the pure natural vegetation (\hat{f}_1) and $2\times\text{CO}_2$ (\hat{f}_3) separate contributions (Figure 2). The other interaction terms (\hat{f}_{12} , \hat{f}_{23} and \hat{f}_{123}) have negligible contributions.

The effect of increased CO_2 concentration was less noticeable on precipitation, except in localized areas in the northern part of the simulation domain. In Brazil precipitation was up to 1mm day^{-1} larger under the natural landscape (i.e. evergreen trees) than under the current agricultural (i.e. corn) conditions (Figure 3). This area of increased rainfall can still be seen in the contributions due to the interaction term \hat{f}_{123} (Figure 3). This is an indication of the complex mechanisms and factors that can be involved in detecting effects on precipitation under future climate conditions (i.e. land-use and higher CO_2 concentrations).

3.2 Sensitivity to future LCC using projected future atmospheric scenarios

Pitman and Narisma (2005) and Narisma and Pitman (2006) addressed the impacts of future LCC, namely reforestation, on the Australian climate. They focused on the potential of reforestation to mitigate the projected summer warming over Australia under two emission scenarios for 2050 and 2100. They performed GEMRAMS ensemble simulations of the January climate over an Australian modeling domain with a 56-km grid spacing. The atmospheric boundary conditions were provided by the Commonwealth Scientific and Industrial Research Organization (CSIRO) Mark 2 atmosphere-ocean model (Watterson and Dix, 2003). Each set of LCC experiments used three types of land-cover scenarios: one current land-cover or steady state (SS or f0 in the FacSep notation), and two reforestation future scenarios (Table 4). In the low reforestation scenario (LCL) a 25% of the area that was converted from Eucalypt trees to grasslands in the last 200 years was recovered. The high reforestation scenario (LCH) recovered at least 75% of the deforested areas. The boundary conditions from the CSIRO model are the 2050 and 2100 projected scenarios combined with a high (A2) and moderate (B2) CO₂ increase scenarios (i.e. 2050B2, 2050A2, 2100B2, 2100A2). This example can be viewed as an application of the "fractional approach of the methodology" (Krichak and Alpert, 2002), with only one varying factor (i.e. LCC). The differences between the LCH, LCL and SS land-cover experiments represent the effects of the "pure" LCC contributions.

The simulations showed that reforestation have the potential to moderate the future warming due to increases in CO₂ concentrations in two of the three regions of LCC. At a continental scale, the overall LCC impact is negligible, but the LCC effects are very clear at a local scale and limited to the areas of the LCC. The patterns of the LCC

impact are also directly associated with the extent of the reforested area: the area of the impact is larger in the LCH case in both 2050 and 2100 scenarios than in the LCL case (Figure 4). Figure 4 also shows that the cooling effect decreased in relative terms as the CO₂ –induced warming intensified, in the A2 scenario and for 2100. The analysis of the near-surface variables showed that the cooling or warming effect of the future LCC is mainly due to changes in the latent heat flux (i.e. increase and decrease respectively) related to increases and reduced LAI values. The results of these simulations show that although the impact of the LCC is at regional scales the effects remain very important given crops, water and habitation exists at these scales.

4. Spatial pattern of land-cover change

Gero and Pitman (2006) used RAMS to assess the impact of land-cover change on a simulated storm event over the Sydney basin in Australia. As urbanization expands, the basin has increasingly transformed into a highly heterogeneous urban area, with agriculture and natural vegetation coexisting within the basin. The summer storms that frequently occur in the Sydney basin can be affected by the presence of the urban surface, suggested by many modeling and observational studies.

The initial experiments set-up used a high-resolution land-cover dataset of the Sydney basin's current land-use pattern and the natural land-cover (i.e. pre-European settlement that occurred in 1778) to explore the potential impact of the LCC over the area. RAMS was configured with four nested grids, with horizontal increments of 60, 12, 3 and 1 km, respectively (Figure 5). The lateral boundary conditions were provided by

the NCEP-NCAR reanalysis as in Eastman et al. (2001) to isolate the effects of LCC on a particular storm event. The natural land-cover was assumed to be homogeneously covered by native bush, primarily 20-m eucalypt forest that still exists in the area. The current land-cover types, generated from satellite images from Landsat 7 Enhanced Thematic Mapper Plus (Figure 5). The land-cover types included three specific urban areas within the Sydney basin (dense urban, new urban, established urban), agricultural land and natural vegetation (bushland). Each of them was associated with specific values in the biophysical parameters.

This initial set of experiments revealed that an intense convective storm developed in the model near Sydney's dense urban central business district under current land-cover, but the storm was absent under natural land-cover conditions (Figure 6). To explore the effect of the dense and new urban surfaces on the generation of the storm under current land-cover, a FacSep approach was implemented using the four current land-cover classes (three urban and agriculture) as factors. All the possible combinations of land-cover in the change from natural to current land-cover, corresponding to 16 possible land-cover maps, were used to performed model simulations with the same NCEP-NCAR atmospheric boundary conditions. For example, Table 5 shows how the land-cover in two of the runs of the factorial analysis was set-up. In run 9, the new urban area was returned to bushland, and in run 10 both new urban and agricultural areas in the current land-cover are returned to bushland. The factorial analysis revealed the storm to be sensitive to the presence of agricultural land in the southwest of the simulation domain (Figure 6). This area, through the roughness length, interacts with the sea breeze and affects the horizontal divergence: the smooth agricultural land exert less drag on the

atmosphere and allowing relative wind acceleration compared to the aerodynamically rough bushland.

5. Model/parameterization improvements vs. better data.

In this last example, RAMS is used to study the relative effects of incorporate a new model parameterization vs. the use of improved data set or boundary conditions. Lei et al (2008) applied the FacSep methodology to study the explicit effects of an urban model and an improved sea surface temperature (SST) data set, as well as their combination effect, on the simulation of a heavy rainfall event over Mumbai with RAMS. They studied a record-breaking event that occurred over Mumbai, India on 25 July 2006 that was poorly represented by operational weather forecasts models. Table 5 shows how the experiments were set up to study the relative impacts of improvements of the model (i.e. incorporation of an urban model) and the use of improved boundary conditions (i.e. observed SST).

Initially, experiments were carried out based on previous evidence that suggests that urban landscape can affect storm morphology. They used RAMS coupled with TEB in the grid cells classified as urban in the innermost simulation domain, while LEAF2 was used as the default land surface scheme in the rest of the grid cells (Figure 7). The experiments are f0 and f2 in Table 6. The urban heat island (UHI) created by the urban landscape helped to generate heavy precipitation over the Mumbai bay area, improving the simulated atmospheric conditions when RAMS without TEB was used.

Prior evidence also suggests that mesoscale boundaries can affect storm-related precipitation and SST pattern is important for coastal city precipitation (Chang et al. 2009; Kumar et al. 2008). To explore the effects of SST as lower mesoscale conditions, a second set of simulations were performed, using the FacSep methodology as basis for the experiments. They used the SST fields from the Tropical Rainfall Measurement Mission (TRMM). Both the sole effects of SST without TEB simulated (\hat{f}_1 in Table 6) and the interactions between TEB and SST (\hat{f}_{12} in Table 6) were simulated. Through the FacSep methodology Lei et al. found that the urban model itself was not the main reason for the better representation of rainfall fields (Figure 7 and 8). The interactions between the UHI simulated by the urban model and the realistic satellite derived SST contributed to accurately position and maintain the convergence zone and the observed heavy precipitation over Mumbai (Figure 9). The local scale heterogeneities generated from the urban landscape and SST interactions, showed here in the convergence fields at 850 hPa (Figure 8,) were a crucial factor that improved the simulated rainfall.

6. Final comments

Examples were presented here of applications of the FacSep methodology using RAMS, a regional mesoscale atmospheric model, for different regions in the world that had experienced important LCC, in addition to the changes in CO₂ levels. We also showed an example of future reforestation and climate scenarios, where the simulations involved the application of the fractional approach of the FacSep methodology.

The FacSep methodology, through these examples, allowed showing the importance of including not only LCC scenarios in future climate change projection simulations but also biological effects of CO₂. This indicates that regional and modeling systems needs to include a land-surface scheme able to represent the processes of photosynthesis and soil and plant respiration, and the allocation of the assimilated carbon to leaves, stems and roots.

Current and future LCC include increases of urban extension. Factorial experiments showed that a particular spatial configuration of a complex urban landscape initiated processes that led to the occurrence of a storm under current land-cover. The presence of agricultural land in a specific area within the simulation domain and not the urban areas themselves triggered the storm. The last example of the application FacSep methodology showed that the interaction between urban parameterization and realistic satellite derived SST improved the location of a storm and the simulation of the associated precipitation. The FacSep methodology was able to identify the important role of the interaction between urban land-cover and the meteorological processes. These results indicate the need to improve the parameterization of not only the particular urban surfaces but also of the other types of land-cover at the periphery of the urban complex areas. In addition, realistic representation of the current land-cover may lead to more accurate weather predictions.

6. Acknowledgments

This work was supported in part by the Shortgrass Steppe Long Term Ecological Research project by funds from the NSF award DEB 0217631, NASA Grant NNX06AG74G and NNX07AG35G, NASA GWEC Grant NNG05GB41G, NOAA JCSDA Grant NA06NES4400013, DOE ARM 08ER64674, NSF Grant ATM-0296159 and ATM 0831331, NSF CAREER ATM-0847472. Roger A. Pielke Sr. was also supported in part by the University of Colorado at Boulder (CIRES/ATOC). Dallas Staley completed the editing of this paper in her usual outstanding manner.

7. References

- Alpert, P., Niyogi, D., Pielke Sr., R.A., Eastman, J.L., Xue, Y.K., and Raman, S. (2006). Evidence for carbon dioxide and moisture interactions from the leaf cell up to global scales: Perspective on human-caused climate change. *Global and Planetary Change*, **54**, 202-208.
- Arora, V.K. (2002). Modeling vegetation as a dynamic component in soil-vegetation-atmosphere-transfer schemes and hydrological models. *Rev. Geophys.* **40**: 100610.1029/2001RG000103.
- Baidya Roy S., Hurtt, G.C., Weaver, C.P., and Pacala, S.W. (2003). Impact of historical land cover change on the July climate of the United States. *J. Geophys. Res.* **108**(D24),4793:doi:10.1029/2003JD003565.
- Ball, J.T., Woodrow, I.E. and Berry, J.A. (1987). A model predicting stomatal conductance and its contribution to the control of photosynthesis under different environmental conditions. *Progress in Photosynthesis Research*, J. Biggins, Ed., Martinus Nijhof Publishers, IV, 221-224.
- Beltrán, A. (2005). Using a coupled biospheric-atmospheric modeling system (GEMRAMS) to model the effects of land-use/land-cover changes on the near surface atmosphere. PhD. Dissertation, 186 pp. Colorado State Univ., Fort Collins, Colorado.
- Beltrán-Przekurat, A., Marshall, C.A. and Pielke Sr., R.A. (2008). Ensemble re-forecasts of recent warm-season weather: Impacts of a dynamic vegetation parameterization. *J. Geophys. Res. - Atmos.*, **113**, D24116, doi:10.1029/2007JD009480.

- Cao, L., Bala, G., Caldeira, K., Nemani, R., and Ban-Weiss, G. (2009). Climate response to physiological forcing of carbon dioxide simulated by the coupled Community Atmosphere Model (CAM3.1) and Community Land Model (CLM3.0). *Geophys. Res. Lett.*, **36**, L10402, doi:10.1029/2009GL037724.
- Castro, C.L., Pielke Sr., R.A. and Leoncini, G. (2005). Dynamical downscaling: assessment of value retained and added using the Regional Atmospheric Modeling System (RAMS). *J. Geophys. Res.*, **110**, D05108, doi:10.1029/2004JDD004721.
- Chase, T.N., Pielke Sr., R.A., Kittel, T.G.F., Zhao, M., Pitman, A.J., Running, S.W. and Nemani, R.R. (2001). The relative climatic effects of landcover change and elevated carbon dioxide combined with aerosols: A comparison of model results and observations. *J. Geophys. Res.*, **106**, 31,685 -31,691.
- Chen, C., and Cotton, W.R.. (1983). A one-dimensional simulation of the stratocumulus capped mixed layer. *Bound.- Layer Meteorol.*, **25**, 298-321.
- Chen, D-X., and Coughenour, M.B. (1994). GEMTM: a general model for energy and mass transfer of land surfaces and its application at the FIFE sites. *Agr. Forest Meteorol.* **68**: 145-171.
- Chen, D-X., and Coughenour, M.B. (2004). Photosynthesis, transpiration, and primary productivity: scaling up from leaves to canopies and regions using process models and remotely sensed data. *Global Biogeochem. Cycles.* **18**:GB4033, doi:10.1029/2002GB001979.
- Chen, D-X., Coughenour, M.B., Knapp, A.K. and Owensby, C.E. (1994). Mathematical simulation of C₄ grass photosynthesis in ambient and elevated CO₂. *Ecol.*

- Modelling*, **73**, 63-80.
- Chen, D-X., Hunt, H.W. and Morgan, J.A. (1996). Responses of a C₃ and C₄ perennial grass to CO₂ enrichment and climate change: comparison between model predictions and experimental data. *Ecol. Modelling*, **87**, 11-27.
- Cotton, W.R., Pielke Sr., R.A., Walko, R.L., Liston, G.E., Tremback, C., Jiang, H., McAnelly, R.L., Harrington, J.Y., Nicholls, M.E., Carrio, G.G. and McFadden, J.P. (2003). RAMS 2001: current status and future directions. *Meteor. Atmos. Phys.*, **82**, 5-29.
- Cotton, W.R., Weaver, J.F. and Beitler, B.A. (1995). An unusual summertime downslope wind event in Fort Collins, Colorado on 3 July 1993. *Wea. Forecasting*, **10**, 786-797.
- De Pury, D.G.G., and Farquhar, G.D. (1997). Simple scaling of photosynthesis from leaves to canopies without the errors of big-leaf models. *Plant Cell Environ.*, **20**, 537-557.
- De Wekker, S.F.J., Steyn, D.G., Fast, J.D., Rotach, M.W., Zhong, S. (2004). The performance of RAMS in representing the convective boundary layer structure in a very steep valley. *Environ. Fluid Mech.* 1–18.
- Douglas, E.M., Niyogi, D., Frolking, S., Yeluripati, J.B., Pielke Sr., R.A., Niyogi, N., Vörösmarty, C.J., and Mohanty, U.C. (2006). Changes in moisture and energy fluxes due to agricultural land use and irrigation in the Indian Monsoon Belt. *Geophys. Res. Lett.* **33**, L14403. doi:10.1029/2006GL026550.
- Douglas E. M., Beltrán-Przekurat, A., Niyogi, D. S., Pielke, Sr., R.A. and Vörösmarty, C. J. (2009). The iImpact of agricultural intensification and irrigation on land-

- atmosphere interactions and Indian Monsoon precipitation - A mesoscale modeling perspective, *Global Planetary Change*, doi:10.1016/j.gloplacha.2008.12.007
- Eastman, J.L., Coughenour, M.B. and Pielke, R.A. (2001). The effects of CO₂ and landscape change using a coupled plant and meteorological model. *Global Change Biology*, **7**, 797-815.
- Farquhar, G.D., von Caemmerer, S. and Berry, J.A. (1980). A biochemical model of photosynthetic CO₂ assimilation in leaves of C₃ species. *Planta*, **149**, 78-90.
- Foley, J.A., DeFries, R., Asner, G.P., Barford, C., Bonan, G., Carpenter, S.R., Chapin, F.S., Coe, M.T., Daily, G.C., Gibbs, H.K., Helkowski, J.H., Holloway, T., Howard, E.A., Kucharik, C.J., Monfreda, C., Patz, J.A., Prentice, I.C., Ramankutty, N., and Snyder, P.K. (2005). Global Consequences of Land Use. *Science*, **309**, 570-574.
- Gero, A. and Pitman, A.J. (2006). The impact of land cover change on a simulated storm event in the Sydney Basin. *J. Applied Meteorology*, **45**, 283-300.
- Goudriaan, J. (1977). *Crop Micrometeorology: A Simulation Study*. Pudoc, 249 pp.
- Harrington, J.Y. (1997). The effects of radiative and microphysical processes on simulated warm and transition season Arctic stratus. Ph.D. Dissertation, 289 pp. Atmospheric Science Paper No 637, Colorado State University, Fort Collins, CO.
- Kain, J.S. (2004). The Kain-Fritsch convective parameterization: an update. *J. Appl. Meteor.*, **43**, 170-181.

- Lawton, R.O., Nair, U.S., Pielke Sr., R.A. and Welch, R.M. (2001). Climatic impact of tropical lowland deforestation on nearby montane cloud forests. *Science*, **294**, 584-587.
- Lei, M., Niyogi, D., Kishtawal, C., Pielke Sr., R.A., Beltrán-Przekurat, A., Nobis, T., and Vaidya, S. (2008). Effect of explicit urban land surface representation on the simulation of the 26 July 2005 heavy rain event over Mumbai, India. *Atmos. Chem. Phys. Discussions*, **8**, 8773–8816.
- Lu, L., and Shuttleworth, W.J. (2002). Incorporating NDVI-Derived LAI into the climate version of RAMS and its impact on regional climate. *J. Hydrometeorol.*, **3**, 347-362.
- Mahrer, Y., and Pielke, R. A. (1977). A numerical study of the airflow over irregular terrain. *Beitrige zur Physik der Atmosphäre*, **50**, 98-113.
- Masson, V. (2000). A physically-based scheme for the urban energy budget in atmospheric models. *Bound.-Layer Meteorol.*, **94**, 357–397.
- Mellor, G.L., and Yamada, T. (1982). Development of a turbulence closure model for geophysical fluid problems. *Rev. Geophys. and Space Phys.*, **20**, 851-875.
- Molinari, J. (1985). A general form of Kuo's cumulus parameterisation. *Mon. Wea. Rev.* **113**, pp. 1411–1416.
- Narisma, G.T., and Pitman, A.J. (2004). The effect of including biospheric responses to CO₂ on the impact of land-cover change over Australia. *Earth Interactions*, **8**, 8-005.

- Narisma G.T. and Pitman, A.J. (2006). Exploring the sensitivity of the Australian climate to regional land-cover change scenarios under increasing CO₂ concentrations and warmer temperatures. *Earth Interactions*, **10**, 1-27. doi:10.1175/EI154.1
- Niyogi D. , Chang, H., Saxena, V. K., Holt, T., Alapaty, K., Booker, F., Chen, F., Davis, K.J., Holben, B., Matsui, T., Meyers, T., Oechel, W.C., Pielke Sr., R. A., Wells, R., Wilson, K. and Xue, Y.K. (2004). Direct observations of the Effects of Aerosol loading on Net Ecosystem CO₂ Exchanges over Different Landscapes, *Geophysical Research Letters*, **31**, L20506, doi:10.1029/2004GL020915.
- Niyogi, D., Alapaty, K., Raman, S. and Chen, F. (2009). Development and Evaluation of a Coupled Photosynthesis-Based Gas Exchange Evapotranspiration Model (GEM) for Mesoscale Weather Forecasting Applications. *J. Appl. Meteor. Climatol.* **48**, 349-368.
- Pielke, R.A. Sr. (2001). Influence of the spatial distribution of vegetation and soils on the prediction of cumulus convective rainfall. *Rev. Geophys.*, **39**, 151-177.
- Pielke Sr. R.A., and Niyogi, D. (2008). The role of landscape processes within the climate system. *In: Otto, J.C. and R. Dikaum, Eds., Landform - Structure, Evolution, Process Control: Proceedings of the International Symposium on Landforms organised by the Research Training Group 437. Lecture Notes in Earth Sciences, Springer, Vol. 115, in press.*
- Pielke, R.A. Sr., W.R. Cotton, R.L. Walko, C.J. Tremback, W.A. Lyons, L.D. Grasso, M.E. Nicholls, M.D. Moran, D.A. Wesley, T.J. Lee, and Copeland, J.H. (1992). A comprehensive meteorological modeling system—RAMS. *Meteor. Atmos. Phys.*, **49**, 69-91.

- Pielke Sr., R.A., Marland, G., Betts, R.A., Chase, T.N., Eastman, J.L., Niles, J.O., Niyogi, D. and Running, S. (2002). The influence of land-use change and landscape dynamics on the climate system- relevance to climate change policy beyond the radiative effect of greenhouse gases. *Phil. Trans. A. Special Theme Issue*. **360**, 1705-1719.
- Pielke, R.A. Sr., J. Adegoke, A. Beltrán-Przekurat, C.A. Hiemstra, J. Lin, U.S. Nair, D. Niyogi, and Nobis, T.E. (2007). An overview of regional land use and land cover impacts on rainfall. *Tellus B*. **59**, 587-601.
- Pitman, A.J. (2003). The evolution of, and revolution in, land surface schemes designed for climate models. *Int. J. Climatol.*, **23**, 479-510.
- Pitman A. J. and Narisma, G. T. (2005). The role of land surface processes in regional climate change: a case study of future land cover change over South Western Australia. *Meteorology and Atmospheric Physics*, **89**, 235-249.
- Rhea, J. O. (1978). Orographic precipitation model for hydrometeorological use. Ph.D. Dissertation, Colorado State University, Department of Atmospheric Science, Ft. Collins, Colorado, p. 198.
- Roy, S. S., Mahmood, R., Niyogi, D., Lei, M., Foster, S. A., Hubbard, K. G., Douglas, E. and Pielke Sr., R.A. (2007). Impacts of the agricultural Green Revolution-induced land use changes on air temperatures in India. *J. Geophys. Res.* **112**, D21108, doi:10.1029/2007JD008834.
- Rozoff, C.M., Cotton, W.R., and Adegoke, J.O. (2003). Simulation of St. Louis, Missouri, Land Use Impacts on Thunderstorms. *J. Appl. Meteor.*, **42**, 716–738.
- Smagorinsky, J. (1963). General circulation experiments with the primitive equations.

- Part I: the basic experiment. *Mon. Wea. Rev.*, **91**, 99-164.
- Solomon, S. et al. (eds) (2007). *Climate Change 2007: The Physical Science Basis. Contribution of Working Group I to the Fourth Assessment Report of the IPCC* (Cambridge Univ. Press, 2007).
- Stein, U. and Alpert, P. (1993) Factor separation in numerical simulations, *J. Atmos. Sci.* **50**, 2107–2115.
- Strack, J.E., Pielke Sr, R.A., Steyaert, L.T. and Knox, R.G. (2008). Sensitivity of June near-surface temperatures and precipitation in the eastern United States to historical land cover changes since European settlement. *Water Resources Research*. **44**, W11401, doi:10.1029/2007WR00654.
- Tremback, C. J. (1990). Numerical simulation of a mesoscale convective complex: model development and numerical results. Ph.D. dissertation, Atmos. Sci. Paper No. 465, Department of Atmospheric Science, Colorado State University, Fort Collins, CO 80523, 247 pp.
- Uppala, S.M., Kållberg, P.W., Simmons, A.J., Andrae, U., Da Costa Bechtold, V., Fiorino, M., Gibson, J.K., Haseler, J., Hernandez, A., Kelly, G.A., Li, X., Onogi, K., Saarinen, S., Sokka, N., Allan, R.P., Andersson, E., Arpe, K., Balmaseda, M.A., Beljaars, A.C.M., Van De Berg, L., Bidlot, J., Bormann, N., Caires, S., Chevallier, F., Dethof, A., Dragosavac, M., Fisher, M., Fuentes, M., Hagemann, S., Hólm, E., Hoskins, B.J., Isaksen, L., Janssen, P.A.E.M., Jenne, R., McNally, A.P., Mahfouf, J.F., Morcrette, J.J., Rayner, N.A., Saunders, R.W., Simon, P., Sterl, A., Trenberth, K.E., Untch, A., Vasiljevic, D., Viterbo, P., Woollen, J. (2005). The ERA-40 re-analysis. *Quarterly J. R. Meteorol. Soc.*, **131**, 2961-3012.

Walko, R.L., Cotton, W.R., Meyers, M.P. and Harrington, J.Y. (1995). New RAMS cloud microphysics parameterization. Part I: the single-moment scheme. *Atmos. Res.*, **38**, 29-62.

Walko, R.L., Band, L.E., Baron, J., Kittel, T.G.F., Lammers, R., Lee, T.J., Ojima, D., Pielke, R.A., Taylor, C., Tague, C., Tremback, C.J. and Vidale, P.L. (2000). Coupled atmosphere-biosphere-hydrology models for environmental modelling. *J. Appl. Meteor.*, **39**, 931-944.

Parameterization	Options	References
Turbulence	Mellor–Yamada; Anisotropic deformation; Isotropic deformation; Deardorff	Mellor and Yamada (1982), Smagorinsky (1963), Cotton et al. (2003)
Radiation	Mahrer–Pielke; Chen–Cotton; Harrington	Mahrer and Pielke (1977), Chen and Cotton (1983), Harrington (1997)
Clouds microphysics	No cloud; condensation only; simple dump-bucket; single-momentum	Walko et al. (1995); Cotton et al. (1995), Rhea (1978)
Convective parameterization	Modified Kuo; Kain-Fritsch	Molinari (1985), Tremback (1990), Kain (2004), Castro et al. (2005)
Surface layer	Specified surface layer gradients; LEAF-2	Walko et al (2000)
Vegetation dynamics	Seasonal and latitudinal leaf area index (LAI) dependence (from climatology); LAI from satellite (climatology or current); prognostic LAI based on daily net carbon assimilation (i.e. GEMRAMS)	Walko et al. (2000); Lu and Shuttleworth (2002); Eastman et al. (2001); Beltrán (2005); Beltrán-Przekurat et al. (2008)
Urban model	RAMS-default urban land-cover; TEB	Walko et al. (2000); Rozoff et al. (2003)

Table 1. Summary of the parameterization options available in RAMS, GEMRAMS and RAMS-TEB.

Exp	Land-cover		CO ₂ radiation		CO ₂ biology		Differences	Contributions from:
	CURR	NAT	CO ₂	2×CO ₂	CO ₂	2×CO ₂		
f0	√		√		√			
f1		√	√		√		$\hat{f}1 = f1 - f0$	Natural vegetation
f2	√			√	√		$\hat{f}2 = f2 - f0$	2 × CO ₂ radiation
f3	√		√			√	$\hat{f}3 = f3 - f0$	2 × CO ₂ biology
f12		√		√	√		$\hat{f}12 = f12 - (f1 + f2) + f0$	Natural vegetation and 2 × CO ₂ radiation
f13		√	√			√	$\hat{f}13 = f13 - (f1 + f3) + f0$	Natural vegetation and 2 × CO ₂ biology
f23	√			√		√	$\hat{f}23 = f23 - (f2 + f3) + f0$	2 × CO ₂ radiation and 2 × CO ₂ biology
f123		√		√		√	$\hat{f}123 = f123 - (f1 + f2 + f3) + (f12 + f13 + f23) - f0$	Natural vegetation and 2 × CO ₂ radiation and 2 × CO ₂ biology

Table 2. Summary of the experiments performed (Exp), the difference fields and their meaning in Eastman et al. (2001) and Beltrán (2005)

		Tmax (°C)	Tmin (°C)	Precip (mm d ⁻¹)
Experiment	f0	23.13	7.30	0.89
Differences	\hat{f}_1	-1.19 (5)	-0.02 (<1)	-0.04 (5)
	\hat{f}_2	0.01 (<1)	0.10 (1)	0.01 (1)
	\hat{f}_3	-0.75 (3)	0.26 (4)	-0.05 (6)
	\hat{f}_{12}	0.03 (<1)	-0.01 (<1)	~ 0
	\hat{f}_{13}	0.07 (<1)	0.07 (1)	~ 0
	\hat{f}_{23}	0.02 (<1)	~ 0	~ 0
	\hat{f}_{123}	0.01 (<1)	~ 0	~ 0

Table 3. Summary of the seasonal and domain averaged daily maximum (Tmax) and minimum temperature (Tmin) and precipitation and contributions from all the factors in the Eastman et al. (2001) sensitivity experiments (see also Table xxxx). Relative changes (x 100) with respect to the control experiment (f0) are shown in parentheses

Exp	Land cover		
	Steady State	LCL	LHC
f0	√		
f1_25		√	
f1_75			√

Table 4. Summary of the experiments performed in Narisma and Pitman (2006) and Pitman and Pitman (2005) for the low (LCL) and high (LHC) reforestation scenarios, for each climate change scenarios (see text).

Exp	Agriculture		Dense urban		New urban		Established urban	
	Yes	No (B)	Yes	No (B)	Yes	No (B)	Yes	No (B)
f0	√		√		√		√	
f1		√		√		√		√
Run 9	√		√			√	√	
Run 10		√	√			√	√	

Table 5. Example of simulations for the factorial experiments in Gero and Pitman (2006). The areas of each type in the current land-cover experiment (Agriculture, Dense urban, New urban, Established urban and Bushland (B) are shown in Figure 5. Simulations f0 and Run 9 generated the storm and f1 and Run 10 did not.

Exp	TEB		SST		Differences	Contributions from:
	No	Yes	Clim	TRMM		
f0	√		√			
f1	√			√	$\hat{f}_1 = f_1 - f_0$	Satellite SST data
f2		√	√		$\hat{f}_2 = f_2 - f_0$	Urban model
f12		√		√	$\hat{f}_{12} = f_{12} - (f_1 + f_2) + f_0$	Urban model and SST data

Table 6. Summary of the experiments performed, the difference fields and their meaning in Lei et al. (2008)

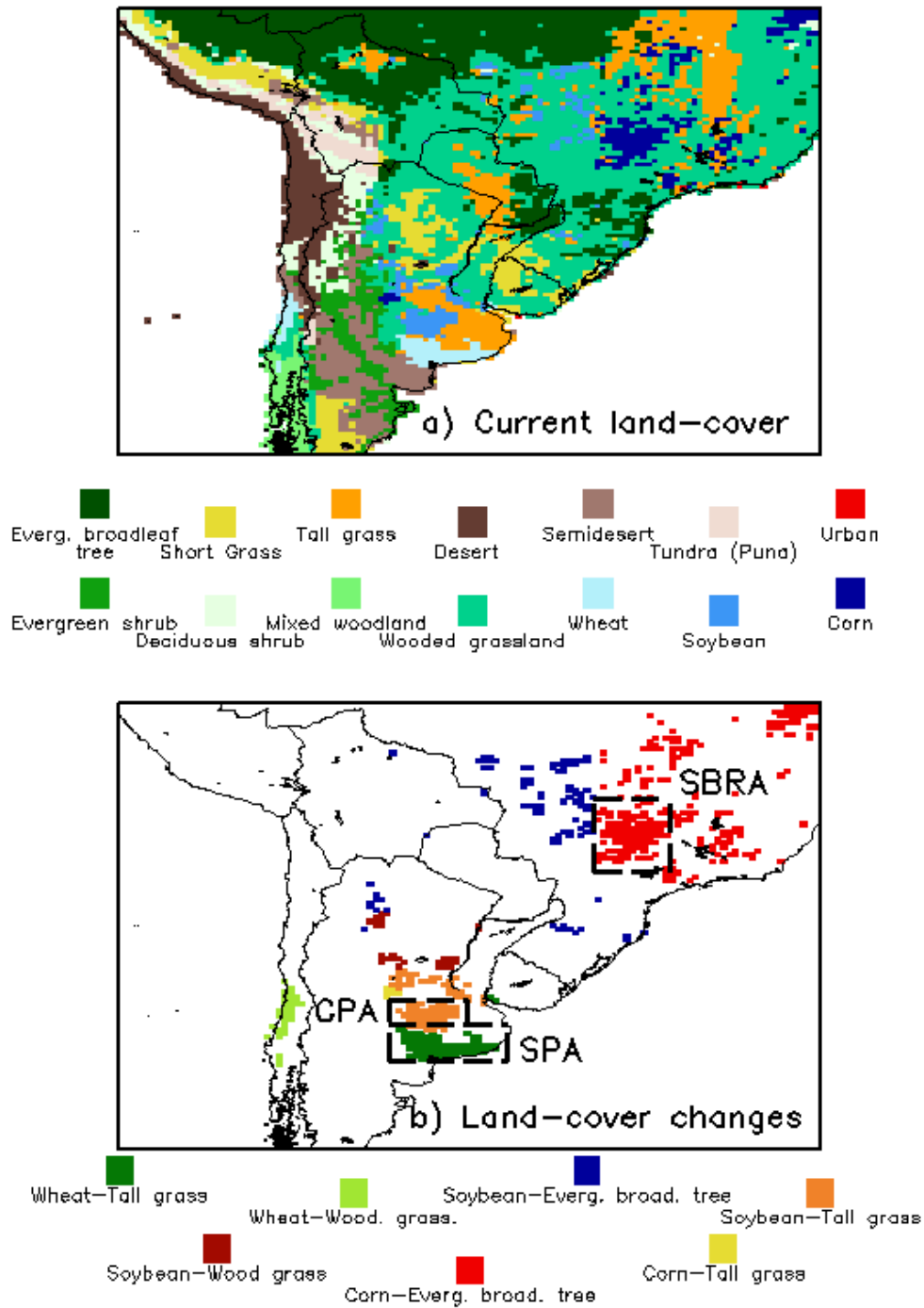


Figure 1. a) Land-cover for the Beltrán (2005) South America simulation domain; b) Land-cover changes in the FacSep methodology RAMS application. CPA: central Pampas; SPA: southern Pampas; SBRA: southern Brazil areas mentioned in the text.

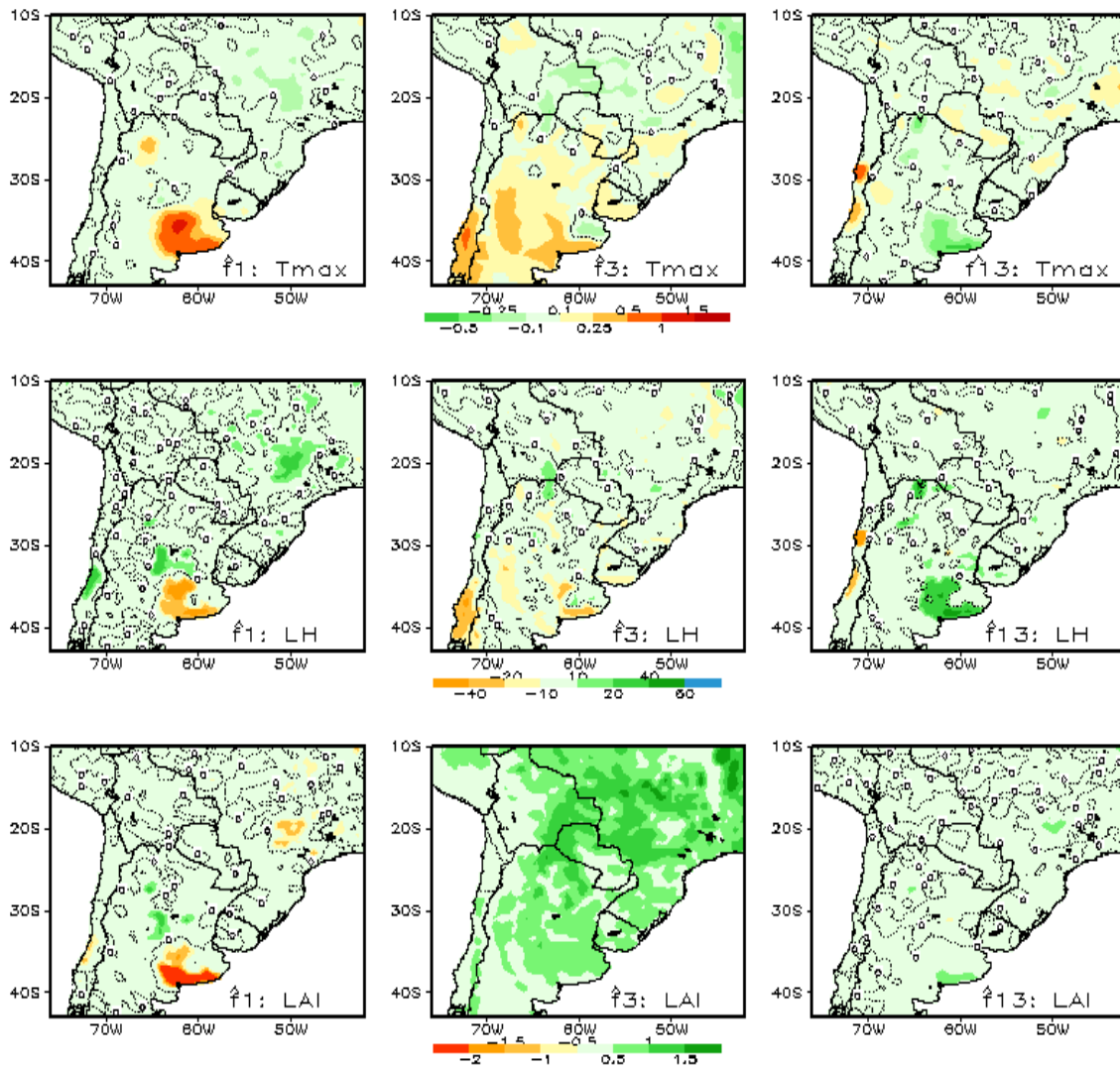


Figure 2. Contributions from natural vegetation, \hat{f}_1 (left); $2xCO_2$ biology, \hat{f}_3 (middle); and both, \hat{f}_{13} (right), for maximum temperature T_{max} ($^{\circ}C$) (top row), diurnal latent heat flux LH (Wm^{-2}) (middle row) and leaf area index LAI ($m^2 m^{-2}$) (bottom row) for the southern South American experiments.

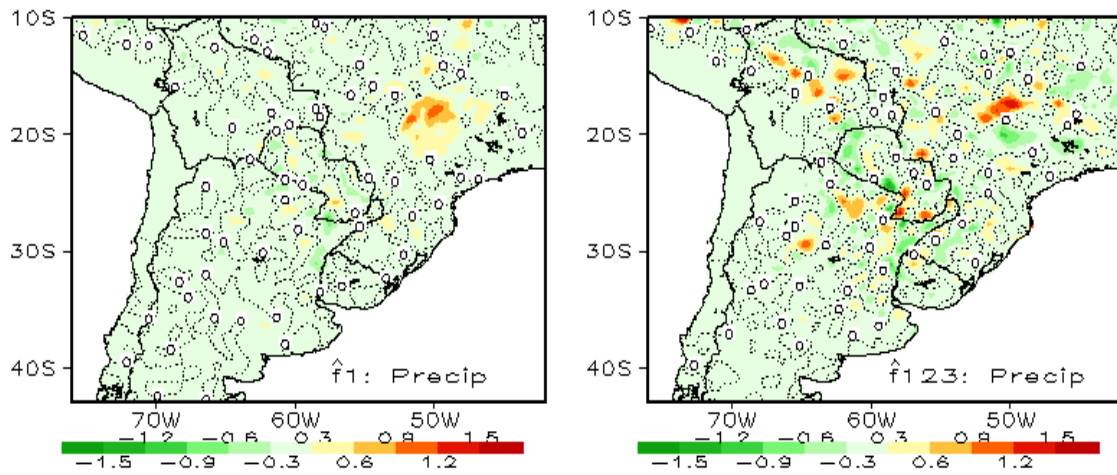


Figure 3. Contributions from natural vegetation, \hat{f}_1 (left) and all natural vegetation, $2\times\text{CO}_2$ biology and $2\times\text{CO}_2$ radiation, \hat{f}_{123} (right) for daily precipitation (mm day^{-1}) for the southern South American experiments.

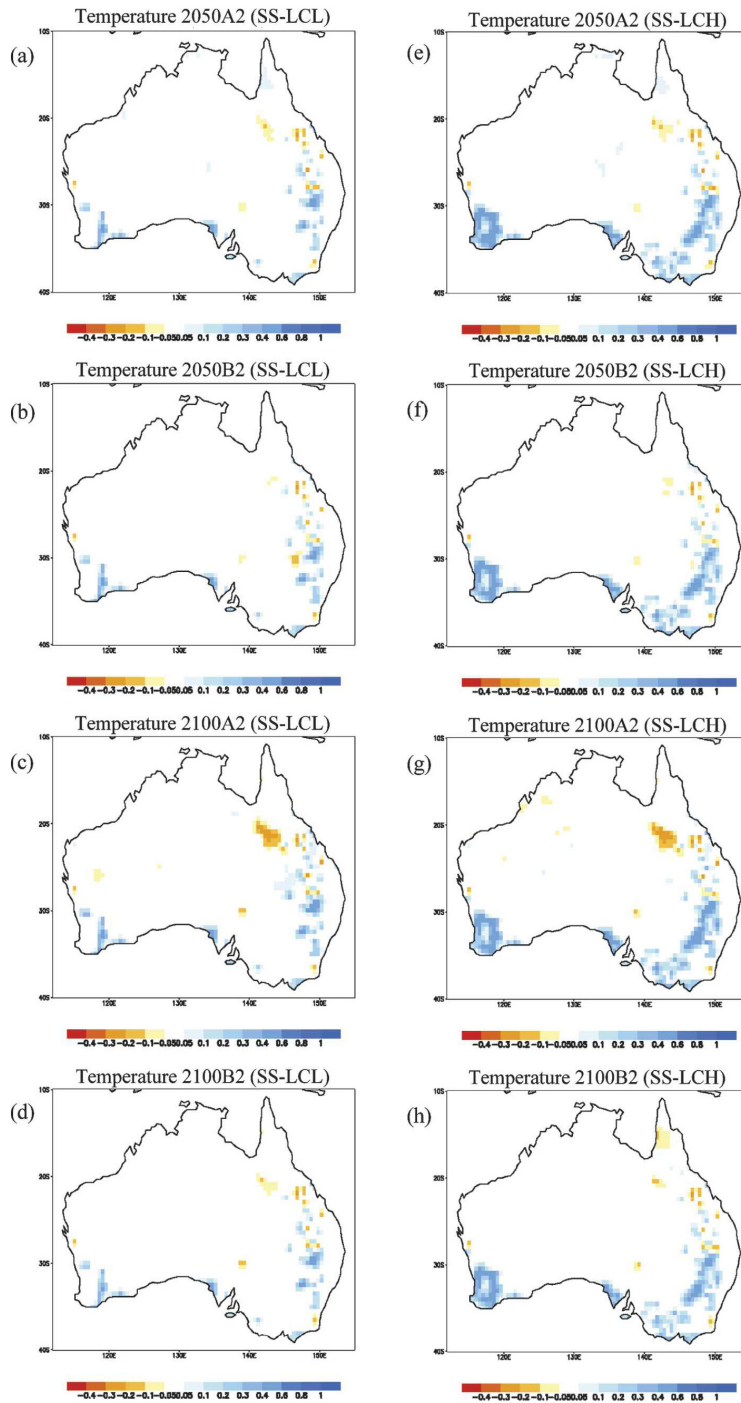


Figure 4. Differences in simulated surface air temperature ($^{\circ}\text{C}$) between SS and LCL (left panels) in a) 2050A2; b) 2050B2; c) 2100A2; d) 2100B2; and between SS and LCH (right panels) in e) 2050A2; f) 2050B2; g) 2100A2; h) 2100B2.

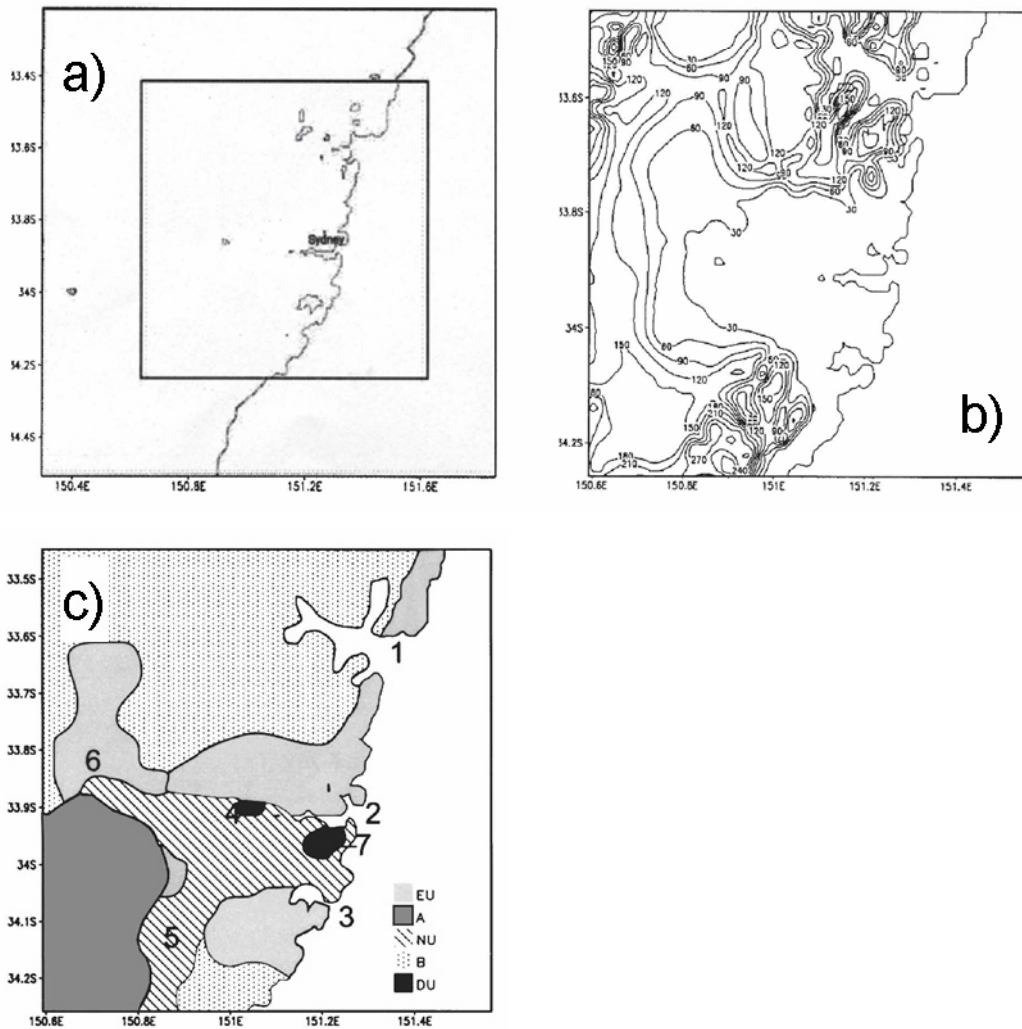


Figure 5. Nesting structure of grids 3 and 4: a) grid 3 with and inset of grid 4; b) grid 4 with topography (meters above sea level); c) current land-cover for grid 4 (EU: established urban, A: agriculture, NU: new urban, B: bushland and DU: dense urban: 1: Broken Bay, 2: Port Jackson, 3: Botany Bay, 4: Parramatta, 5: Campbelltown and 6: Penrith). (From Gero and Pitman, 2006).

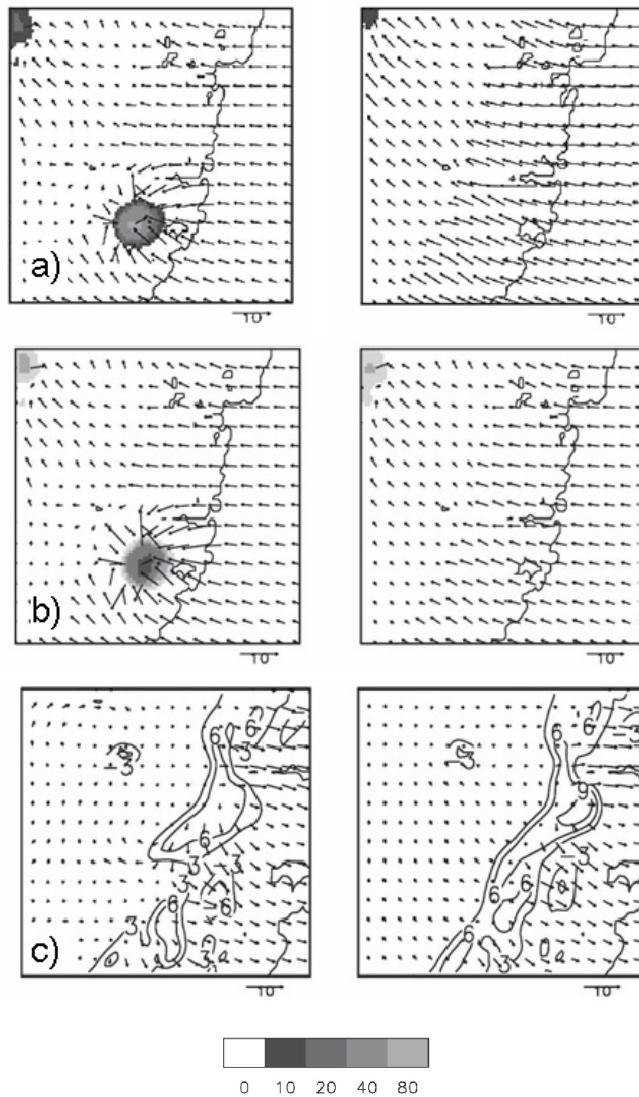
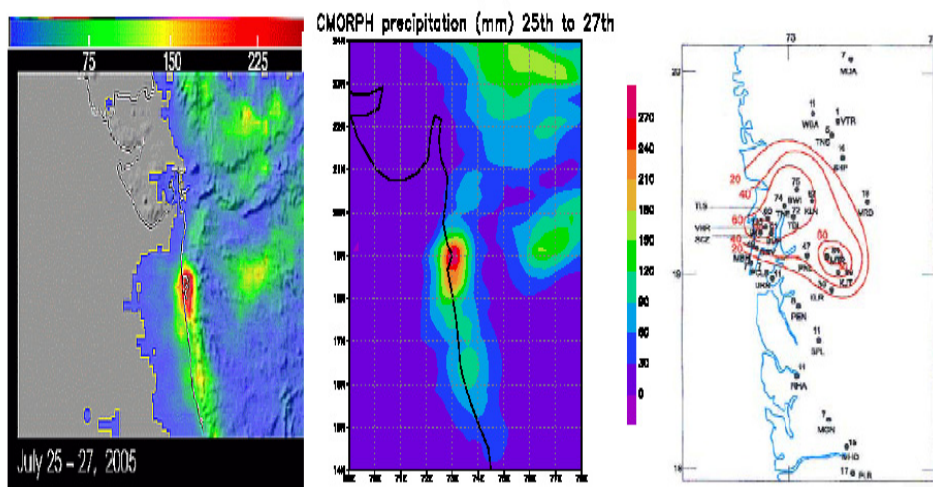


Figure 6. Simulated storm in grid 4 showing precipitation rate (gray shades; mm h^{-1}) and surface winds (arrowed vectors; m s^{-1}) at 1415 LST for a) (left) current and (right) natural land-cover conditions and b) (left) Run 9 and (right) Run10 of the factorial simulations (See Table xxx). c) Horizontal divergence (10^4 s^{-1}) and winds at 850 hPa prior to the storm for (left) Run 9 and (right) Run10 of the factorial simulations.



a). TMI precipitation (mm) b). CMORPH (mm) c). Gauge data (cm)

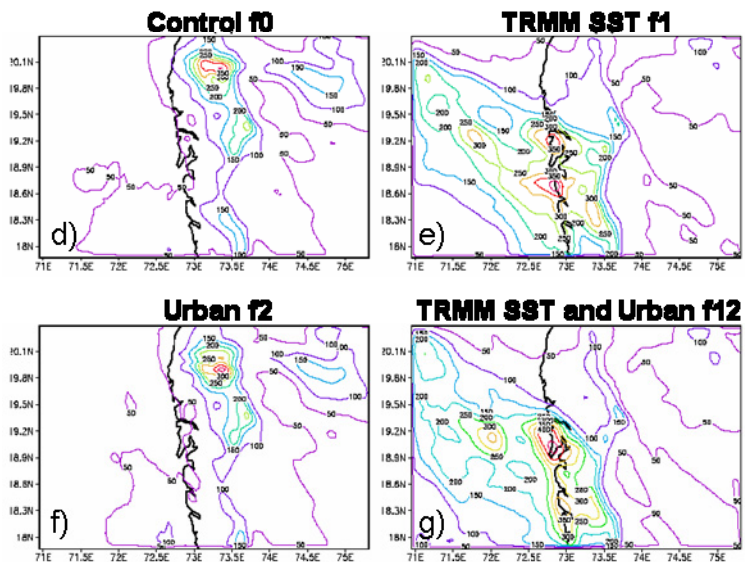


Figure 7. Total precipitation (mm) from different sources and from FacSep analysis experiments: a) TRMM; b) CMORPH; c) gauge data; d) Control, f0; e) TRMM SST, f1; f) Urban TEB, f2; g) TRMM SST and Urban, f12.

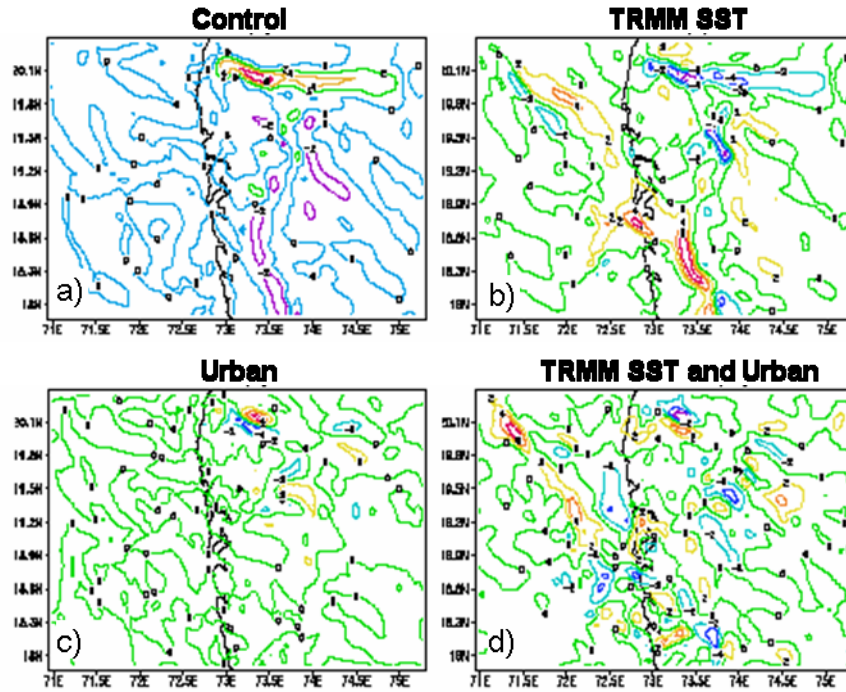


Figure 8. Factor separation values of single and interaction effects for the 850 hPa convergence (10^{-4} s^{-1}) on 09Z July 26: a) Control experiment, \hat{f}_0 ; b) Contribution from satellite SST data, \hat{f}_1 ; c) Contribution from the urban model, \hat{f}_2 ; d) contribution from both the satellite SST data and the urban model, \hat{f}_{12}

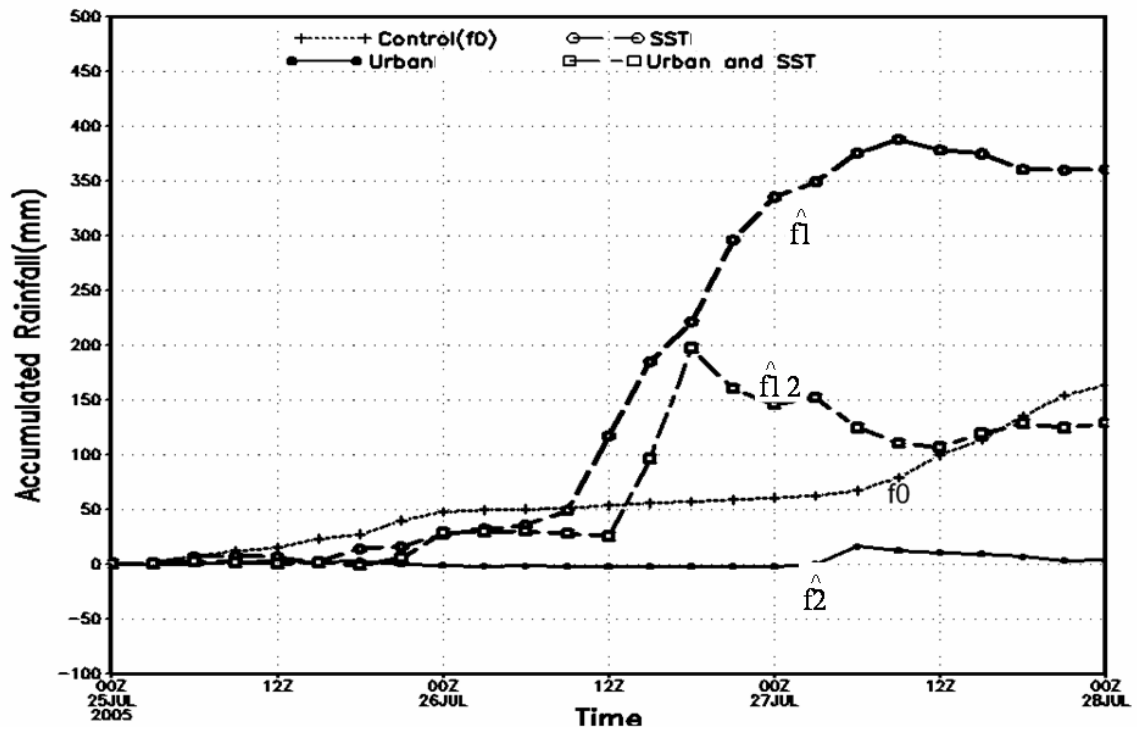


Figure 9. Analysis of the time series accumulated precipitation (mm) over Santacruz airport: the control, the effect of TRMM SST, the effect of urban model and the effect of their interactions.